Supplementary Material to the article

“Casimir–Lifshitz friction force and kinetics of radiative heat transfer of metal plates in relative motion”

When calculating integrals in (2), (3), (5)–(7), it is convenient to introduce a new frequency variable $\omega = \nu_m(T_1, T_2)t$, with $\nu_m(T_1, T_2) = \max(\nu_1(T_1),\ \nu_2(T_2))$ and $\nu_i(T_i)$ being the relaxation frequencies of plates 1 and 2 depending on their temperatures T_1 and T_2 $(i = 1, 2)$. The 2D wave-vector modulus (we use polar coordinates (k, ϕ) in the plane (k_x, k_y)) is expressed as $k = (\omega_p/c)\sqrt{y^2 + \beta_m^2 t^2}$ in evanescent sector $k > \omega/c$ and $k = (\omega_p/c)\sqrt{\beta_m^2 t^2 - y^2}$ in radiation sector $k < \omega/c$, with additional parameters $\beta_m = \nu_m/\omega_p$, $\alpha_i = \hbar\nu_i/T_i$, $\gamma_i = \nu_i/\nu_m$, $\lambda = \omega_p a/c$, $\zeta = (V/c)\beta_m^{-1}$ and $K = \hbar\nu_m^2(\omega_p/c)^4/2\pi^2$. With these definitions, for $k > \omega/c$, formulas (2), (3) and (5) take the form

$$P_1 = K\int_0^\infty dt \int_0^\infty dy y^3 f_1(t, y), \tag{S1}$$

$$P_2 = -K\int_0^\infty dt \int_0^\infty dy y^3 f_2(t, y), \tag{S2}$$

$$F_x V = -K\int_0^\infty dt \int_0^\infty dy y^3 f_3(t, y), \tag{S3}$$

$$f_1(t, y) = t\int_0^\pi d\phi \frac{\mathrm{Im} w_1 \mathrm{Im} w_2}{|D|^2} Z(t, y, \phi), \tag{S4}$$

$$f_2(t, y) = \int_0^\pi d\phi t^- \frac{\mathrm{Im} w_1 \mathrm{Im} w_2}{|D|^2} Z(t, y, \phi), \tag{S5}$$

$$f_3(t, y) = \zeta\int_0^\pi d\phi \cos\phi\sqrt{y^2 + \beta_m^2 t^2}\, \frac{\mathrm{Im} w_1 \mathrm{Im} w_2}{|D|^2} Z(t, y, \phi). \tag{S6}$$

$$Z(t, y, \phi) = \coth\left(\frac{\alpha_1 t}{2}\right) - \coth\left(\frac{\alpha_2 t^-}{2}\right), \tag{S7}$$

$$w_1 = \sqrt{y^2 + \frac{t}{t + \mathrm{i}\cdot\gamma_1}},\quad w_2 = \sqrt{y^2 + \frac{t^-}{t^- + \mathrm{i}\cdot\gamma_2}},\quad t^- = t - \zeta\cos\phi\sqrt{y^2 + \beta_m^2 t^2}, \tag{S8}$$

$$D = (y + w_1)(y + w_2)\exp(\lambda y) - (y - w_1)(y - w_2)\exp(-\lambda y). \tag{S9}$$

For $k < \omega/c$, formulas (S8), (S9) should be used with the replacements $y \to \mathrm{i}\cdot y$, and the substitution of $\beta_m t$ for ∞ in the integrals over y in (S1)–(S3).

In the case $T_1 = T_2 = 0$, Eq. (7) reduces to (only evanescent waves contribute)

$$F_x = \frac{\hbar\nu_0}{\pi^2}\left(\frac{\omega_p}{c}\right)^3 \int_0^\infty dy y^3 \int_0^{\frac{\pi}{2}} d\phi\cos\phi \int_0^{\tau(y,\phi)} dt\sqrt{y^2 + \beta_m^2 t^2}\, \frac{\mathrm{Im} w_1 \mathrm{Im} w_2}{|D|^2}, \tag{S10}$$

where $\tau(y,\phi) = \zeta y\cos\phi/\sqrt{1-\beta_m^2\zeta^2\cos^2\phi}$ and ν_0 is the relaxation frequency corresponding to residual resistance $\rho_0 = 4\pi\nu_0/\omega_p^2$. For identical plates, in the limit $V\to 0$, Eq. (7) and (S10) can be simplified further. Really, in (S8), for $\mathrm{Im}w_1$, one obtains (the final approximation holds for $0 < t \ll y < \infty$)

$$\mathrm{Im}w_1 = \frac{(\sqrt{(t^2+[y^2+t^2(1+y^2)]^2} - y^2 - t^2(1+y^2))^{1/2}}{\sqrt{2(1+t^2)}} \approx \frac{t}{2y}, \tag{S11}$$

while $\mathrm{Im}w_2$ is determined by the same Eq. (S11) when replacing $t \to t^-$. Moreover, $\tau(y,\phi) \cong \zeta y\cos\phi$ and $|D|^2 \cong 16y^4\exp(2\lambda y)$. Then the dimensionless integral in (S10) takes the form

$$I \approx \frac{1}{64}\int_0^\infty dyy^{-1}\exp(-2\lambda y)\int_0^{\frac{\pi}{2}} d\phi\cos\phi \int_0^{\zeta y\cos\phi} dtt(t-\zeta y\cos\phi) = -\frac{\pi}{2^{12}}\frac{\zeta^3}{\lambda^2}. \tag{S12}$$

Inserting (S12) into (S10) yields Eq. (8).

In the case $T_1 = T_2 = T$, using the same notation, Eq. (6) takes the form [19, 20]

$$F_x = -\frac{\hbar V}{8\pi^2}\left(\frac{\omega_p}{c}\right)^4 \frac{1}{\alpha} I_m, \tag{S13}$$

$$I_m = \alpha^2 \int_0^\infty \frac{dt}{\sinh(\alpha t/2)^2}\int_0^\infty dyy^3(y^2+\beta_m^2 t^2)\frac{(\mathrm{Im}w_1)^2}{|D|^2}, \tag{S14}$$

where $|D|$ and $\mathrm{Im}w_1$ are given by (9), (10); $\beta_m = \nu(T)/\omega_p$ and $\alpha = \hbar\nu(T)/T$. It is the dependence $F_x \propto 1/\alpha$ in (S13) that yields a large enhancement of friction at $T\to 0$ for $\alpha \ll 1$, since I_m weakly depends on α, and $\nu(T) = \rho(T)\omega_p^2/4\pi$ decreases with decreasing temperature (see Fig. S1).

To verify this, we consider in (S14) the integration domain $0 < t \ll y$, $p < y < \infty$, where $p \sim 1$ is a constant. In this case, it follows $\alpha^2\sinh(\alpha t/2)^{-2} \approx 4/t^2$, $(\mathrm{Im}w_1)^2 \approx t^2/4y^2$, $|D|^2 \approx 16y^4\exp(2\lambda y)$. Inserting these relations into (S14) yields the assessment

$$I_m > \frac{1}{16}\int_0^p dt \int_p^\infty dy\frac{\exp(-2\lambda y)}{y} = -\frac{p}{16}Ei(-2\lambda p), \tag{S15}$$

with $Ei(-x)$ being the integral exponential function. As follows from the numerical computation, Eq. (S15) yields the essential part of the integral in (S14).

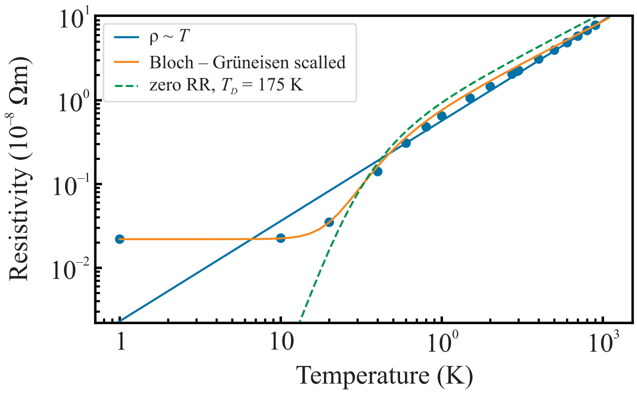

Fig. S1. Au resistivity [26]

Table S1. Friction coefficient of gold plates depending on temperature T and gap width a in models BG and BGM ($V = 1\,\mathrm{m/s}$)

T, K	η, BG $(\mathrm{kg/m^2 \cdot s})$			η, BGM $(\mathrm{kg/m^2 \cdot s})$		
a, nm	10	15	20	10	15	20
1	$1.53 \cdot 10^{-5}$	$1.13 \cdot 10^{-5}$	$8.69 \cdot 10^{-6}$	$1.76 \cdot 10^{-7}$	$1.16 \cdot 10^{-7}$	$8.80 \cdot 10^{-8}$
2	$8.27 \cdot 10^{-4}$	$6.08 \cdot 10^{-4}$	$4.63 \cdot 10^{-4}$	$3.84 \cdot 10^{-7}$	$2.58 \cdot 10^{-7}$	$1.88 \cdot 10^{-7}$
3	$3.46 \cdot 10^{-3}$	$2.44 \cdot 10^{-3}$	$1.80 \cdot 10^{-3}$	$5.88 \cdot 10^{-7}$	$3.95 \cdot 10^{-7}$	$2.87 \cdot 10^{-7}$
5	$1.08 \cdot 10^{-3}$	$7.25 \cdot 10^{-4}$	$5.26 \cdot 10^{-4}$	$9.69 \cdot 10^{-7}$	$6.49 \cdot 10^{-7}$	$4.70 \cdot 10^{-7}$
10	$6.74 \cdot 10^{-5}$	$4.51 \cdot 10^{-5}$	$3.28 \cdot 10^{-5}$	$1.77 \cdot 10^{-7}$	$1.18 \cdot 10^{6}$	$8.59 \cdot 10^{-7}$
15	$1.35 \cdot 10^{-5}$	$9.03 \cdot 10^{-6}$	$6.55 \cdot 10^{-6}$	$2.44 \cdot 10^{-6}$	$1.63 \cdot 10^{-6}$	$1.18 \cdot 10^{-6}$
20	$4.76 \cdot 10^{-6}$	$3.19 \cdot 10^{-6}$	$2.31 \cdot 10^{-6}$	$2.23 \cdot 10^{-6}$	$1.49 \cdot 10^{-6}$	$1.08 \cdot 10^{-6}$
50	$6.41 \cdot 10^{-7}$	$4.30 \cdot 10^{-7}$	$3.12 \cdot 10^{-7}$	$8.05 \cdot 10^{-7}$	$5.94 \cdot 10^{-7}$	$3.92 \cdot 10^{-7}$
100	$4.07 \cdot 10^{-7}$	$2.71 \cdot 10^{-7}$	$1.98 \cdot 10^{-7}$	$5.55 \cdot 10^{-7}$	$3.72 \cdot 10^{-7}$	$2.71 \cdot 10^{-7}$
200	$3.59 \cdot 10^{-7}$	$2.39 \cdot 10^{-7}$	$1.74 \cdot 10^{-7}$	$4.47 \cdot 10^{-7}$	$3.00 \cdot 10^{-7}$	$2.19 \cdot 10^{-7}$
300	$3.50 \cdot 10^{-7}$	$2.33 \cdot 10^{-7}$	$1.70 \cdot 10^{-7}$	$4.38 \cdot 10^{-7}$	$2.94 \cdot 10^{-7}$	$2.14 \cdot 10^{-7}$

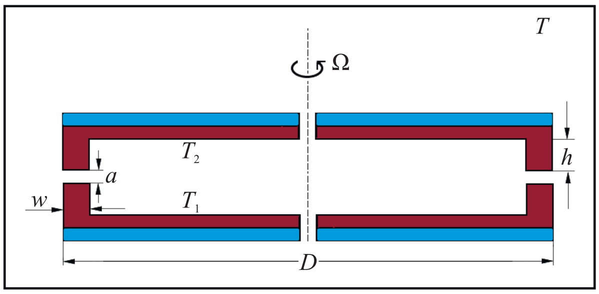

Fig. S2. The proposed setup (side view) for measuring Casimir–Lifshitz friction force. The top plate (disk) can rotate with an angular velocity Ω. On the outer side, the disks have a heat-shielding coating, and on the inner side, they have a metal coating over the entire area with an annular protrusion having a height h and a width $w \ll D$ in the peripheral region. The protruding annular parts of the discs are in vacuum contact with an adjustable gap width $a \ll h$. When the upper disk rotates, its annular surface moves with a linear velocity $V = \Omega D/2$. Heating is carried out by near-field modes in the region of the annular protrusions. The contributions from the portions of the plates located at a distance $a + 2h$ are negligibly small. The temperature control of immovable disk 1 is provided by a thermal sensor. At rotation frequencies $n = 1 \div 10^4$ rps and disk diameter $D = 0.1\,\mathrm{m}$, the investigated speed range will be $0.3 \div 3000\,\mathrm{m/s}$. The optimal scenario for measurements seems to be the quasi-stationary temperature regime, when the temperatures of the disks increase at the same rate from the initial temperature T_0. The time of heating can be varied in a wide range by changing the velocity V, distance a, geometric dimensions and material properties of the plates